

Spin-Wave Instabilities and Non-Collinear Magnetic Phases of a Geometrically-Frustrated Triangular-Lattice Antiferromagnet

J.T. Haraldsen,¹ M. Swanson,^{1,2} G. Alvarez,³ and R. S. Fishman¹

¹*Materials Science and Technology Division, Oak Ridge National Laboratory, Oak Ridge, TN 37831*

²*Department of Physics, North Dakota State University, Fargo, ND 58105 and*

³*Computer Science & Mathematics Division and Center for Nanophase Materials Sciences, Oak Ridge National Laboratory, Oak Ridge, TN 37831*

This paper examines the relation between the spin-wave instabilities of collinear magnetic phases and the resulting non-collinear phases for a geometrically-frustrated triangular-lattice antiferromagnet in the high spin limit. Using a combination of phenomenological and Monte-Carlo techniques, we demonstrate that the instability wave-vector with the strongest intensity in the collinear phase determines the wave-vector of a cycloid or the dominant elastic peak of a more complex non-collinear phase. Our results are related to the observed multi-ferroic phase of Al-doped CuFeO_2 .

PACS numbers: 75.30.Ds, 75.50.Ee, 61.05.fg

It is well-known that the transition between different magnetic ground states may be signaled by the softening of a spin-wave (SW) mode. In the simplest case of a conventional square-lattice antiferromagnet, the softening of a SW mode at wave-vectors $(\pi, 0)$ and $(0, \pi)$ signals the spin flop and canting of the magnetic moments at a critical field. In the manganites [1], the SW instabilities of the ferromagnetic state have been used to construct the phase diagram for the antiferromagnetic (AF) phases that appear with Sr doping. The softening of a SW excitation at $(\pi, 0)$ signals the instability of the Néel state and the canting of the spins in a spin-1/2 union-jack lattice [2]. But the relation between the SW instabilities of a collinear phase and a resulting non-collinear phase is less clear when multiple SW instabilities occur simultaneously or when the non-collinear phase has a complex magnetic structure with several elastic peaks. This paper explores the relation between the SW instabilities of the collinear 4 and 8-sublattice (SL) phases of a geometrically-frustrated triangular-lattice antiferromagnet (TLA) and the non-collinear phases that appear with decreasing anisotropy D . When multiple SW instabilities of the collinear phase occur at once, the instability wave-vector with the largest intensity determines the dominant ordering wave-vector of the resulting non-collinear phase. One of the predicted non-collinear phases may be related to the multi-ferroic phase that appears in CuFeO_2 with Al doping [3].

Frustrated TLAs with AF nearest-neighbor exchange $J_1 < 0$ exhibit a remarkable number of competing ground states [4]. With interactions J_i up to third nearest neighbors (denoted in Fig. 1) and assuming Ising spins along the \mathbf{z} direction, Takagi and Mekata [5] obtained a phase diagram with ferromagnetic (FM), 2-SL, 3-SL, 4-SL, and 8-SL phases. A portion of that phase diagram is sketched in Fig. 1. For the geometrically-frustrated TLA CuFeO_2 in fields below 7 T, the ground state is the 4-SL phase [6, 7] and the black dot in Fig. 1 denotes the estimated ratio of exchange parameters $J_2/|J_1| \approx -0.44$ and

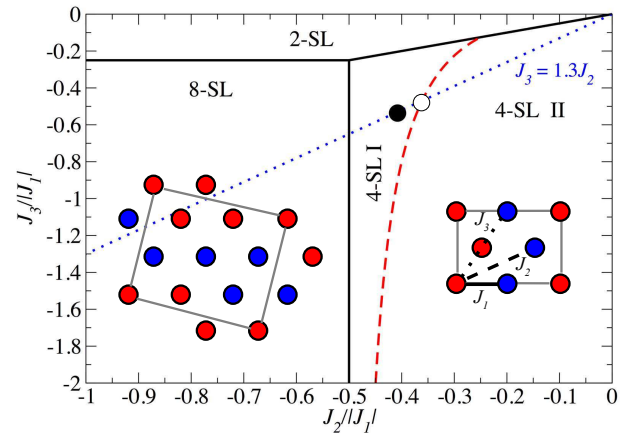


FIG. 1: (Color online) A portion of the TLA phase diagram for large D and $J_1 < 0$. The dashed (red) curve divides the 4-SL phase into 4-SL I and 4-SL II regions. For the 4 and 8-SL phases, red circles denote up spins and blue circles denote down spins; the solid (gray) line defines the unit cell. The dashed (blue) line obeys the relation $J_3 = 1.3J_2$, the black circle is the estimated location of the exchange parameters for CuFeO_2 , and the white circle lies on the boundary between the 4-SL I and 4-SL II regions.

$$J_3/|J_1| \approx -0.57 \text{ [8, 9].}$$

As demonstrated by the small SW gap of about 0.9 meV [3, 8] on either side of the ordering wave-vector $\mathbf{q} = \pi\mathbf{x}$, the spin fluctuations of CuFeO_2 are much softer than would be expected for Ising spins. With Heisenberg spins, the collinear magnetic phases of a TLA become locally unstable below a critical anisotropy D_c that depends on the exchange parameters J_i . The observed softening of the SW modes in $\text{CuFe}_{1-x}\text{Al}_x\text{O}_2$ with Al doping [3] can be reproduced by lowering D towards D_c [10] in the 4-SL I region of Fig. 1. For Al concentrations above about $x_c \approx 0.016$, the magnetic ground state of $\text{CuFe}_{1-x}\text{Al}_x\text{O}_2$ becomes non-collinear and dis-

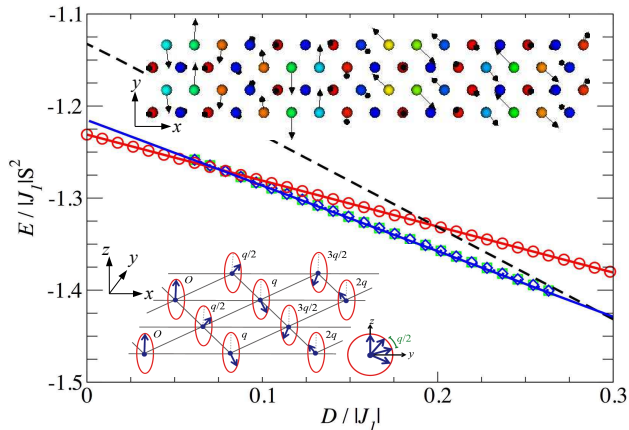


FIG. 2: (Color online) Energy as a function of $D/|J_1|$ for the 4-SL (black dashed), CNC (blue diamonds), and cycloid I (red circles) phases with $J_3/J_2 = 1.3$ and $J_1/J_2 = 2.28$. The bottom diagram shows the cycloid for arbitrary q . The top diagram shows the CNC phase with up spins in red and down spins in blue.

plays multi-ferroic properties [11, 12, 13].

We have determined the ground-state magnetic phases of the TLA using a combination of Monte-Carlo (MC) simulations and phenomenological techniques. The TLA Hamiltonian is

$$H = -\frac{1}{2} \sum_{i \neq j} J_{ij} \mathbf{S}_i \cdot \mathbf{S}_j - D \sum_i S_{iz}^2, \quad (1)$$

where J_{ij} includes first, second, and third-neighbor interactions (shown in Fig. 1). The nearest-neighbor distance has been set to 1. The SW frequencies of the collinear phases are obtained by performing a Holstein-Primakoff $1/S$ expansion about the classical limit. Above the critical anisotropy D_c , a collinear phase is locally stable if the SW frequencies $\omega(\mathbf{k})$ are positive and real for every momentum \mathbf{k} .

MC simulations were used to find the non-collinear magnetic phases of the TLA. The simulations were started at a high-enough temperature to rule out metastable states. To mimic the process of thermal annealing, the system was slowly cooled to a final temperature (in units of $|J_1|S^2$) ranging from 4×10^{-3} to 1×10^{-4} . Lowering the final temperature further did not significantly change the resulting non-collinear phase. Using lattices of varying sizes with periodic boundary conditions, we found that there was no substantial change for lattices greater than 16×16 .

In Fig. 1, the 4-SL phase is separated into regions I and II by the curve $J_1/J_2 - 2 = J_2/J_3$. In region 4-SL II, the instability wave-vectors are given by $\mathbf{k} = (\pi \pm \pi/3)\mathbf{x}$, independent of the exchange parameters; in region 4-SL I, the instability wave-vectors depend on the exchange

parameters [14]. With the exchange parameters corresponding to the black circle in region 4-SL I, we determined the stable magnetic phases as a function of D . As shown in Fig. 2, the 4-SL phase is stable down to $D/|J_1| \approx 0.27$, below which MC simulations obtain the complex non-collinear (CNC) phase shown on the top of Fig. 2. Since the same up or down spin frequently occurs at sites $\mathbf{R} = m\mathbf{x} + n\sqrt{3}\mathbf{y}$ and $\mathbf{R}' = \mathbf{R} + \mathbf{x}/2 + \sqrt{3}\mathbf{y}/2$ or $\mathbf{R}'' = \mathbf{R} - \mathbf{x}/2 + \sqrt{3}\mathbf{y}/2$, the CNC phase retains some of the FM correlations present in the 4-SL phase. Translationally invariant in the \mathbf{y} direction, the CNC phase has a period in the \mathbf{x} direction between 2 and 3 lattice constants. Because the MC simulations were performed on a finite lattice, the energy of the CNC phase is overestimated and we cannot say whether this phase is commensurate or incommensurate.

Below a second threshold value of $D/|J_1| \approx 0.08$, a cycloid like the one sketched in the bottom panel of Fig. 2 [15] has a lower energy than the CNC phase. As discussed below, the wave-vector of the cycloid is independent of D . If the CNC phase were neglected, then the cycloid would achieve a lower energy than the 4-SL phase below $D/|J_1| \approx 0.2$, still above the critical value $D_c/|J_1| \approx 0.15$ for the local stability of the 4-SL phase.

To gain a better understanding of the phases stabilized within the TLA, we have evaluated the magnetic phases along the line with $J_3/J_2 = 1.3$ drawn through the black dot in Fig. 1. Five stable phases are presented as a function of $|J_1|/D$ and $|J_2|/D$ in Fig. 3. The 4-SL phase is stable along a strip through the diagonal of this plot. Although not indicated by this figure, the 4-SL region disappears above $|J_1|/D \approx 40$. Close to the origin or for large D , a collinear 8-SL region is indicated in Fig. 1. Two cycloids are also obtained: in the upper left, cycloid II with wave-vector $4\pi\mathbf{x}/3$; in the lower right, cycloid I with the variable wave-vector indicated in the figure [15]. Finally, a CNC phase appears just below the 4-SL phase and disappears above $|J_1|/D \approx 20$. Regions of local stability for the collinear phases are indicated in Fig. 3 by the dashed black lines [14]. The results in Fig. 2 can be obtained from Fig. 3 by drawing a line from the origin with slope 2.28 (gray) (so that $J_2/|J_1| = -0.44$), which passes from the 4-SL phase through the CNC phase into cycloid I.

The classical energies of each of these phases can be written as $E/S^2 = A_1J_1 + A_2J_2 + A_3J_3 - A_D D$. The coefficients for each phase are given in Table I. Only a non-collinear phase with $0.5 < A_D < 1$ can intercede between a collinear phase with $A_D = 1$ and a cycloid with $A_D = 0.5$. For the CNC phase with $A_D \approx 0.71$, the error bars indicate the range of parameters obtained from MC simulations near $|J_1|/D = 5.7$ and $|J_2|/D = 2.5$. This phase is characterized by rather weak next-neighbor correlations with small $|A_2|$. The CNC phase space in Fig. 3 is obtained by using the results of Table I to evaluate the energies of the MC spin configurations as

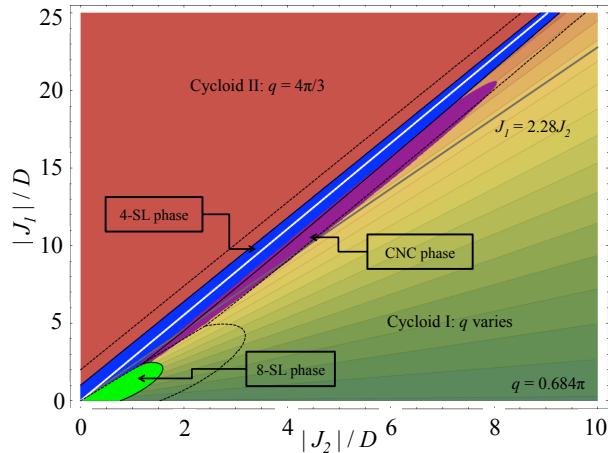


FIG. 3: (Color online) Phase diagram for the TLA as a function of $|J_1|/D$ and $|J_2|/D$ with $J_3 = 1.3J_2$ containing five regions: 4-SL (blue), 8-SL (green), CNC (violet), cycloid I (variable green-orange), and cycloid II (maroon). The dashed (white) line separates regions 4-SL I and 4-SL II. The dotted (black) curves denote the metastable boundaries for the 4-SL and 8-SL regions. Cycloid I has wave-vectors q that range from 0.684π to 0.923π in intervals of 0.016π .

functions of $|J_1|/D$ and $|J_2|/D$. Hence, the CNC region may be *underestimated*.

The ordering wave-vector $\mathbf{q} = q\mathbf{x}$ of cycloid I is evaluated by minimizing E with respect to q . So q depends only on the ratios J_2/J_1 and J_3/J_2 , as indicated by the diagonal lines in Fig. 3. Cycloid II with $q = 4\pi/3$ corresponds to the 120° Néel state found in a classical TLA with $D = 0$ and nearest and next-nearest neighbor interactions [16] when $|J_2/J_1| < 1/8$. A slightly distorted Néel state [15] is stable for nonzero D over a range of exchange parameters with $|J_3/J_2| > 1/2$, so that the diagonal line in Fig. 1 passes through the 4-SL and 8-SL phases. MC simulations were used to confirm the stability of cycloids I and II in Fig. 3.

With decreasing D or moving away from the origin of Fig. 3 along a diagonal, the 4-SL phase becomes unstable either to cycloid II or to the CNC phase. The white line bisecting region the 4-SL strip in Fig. 3 corresponds to the white point in Fig. 1 at the border between the 4-SL I and 4-SL II regions with $J_2/J_1 = -0.36$. In region 4-SL II or above the white diagonal line, the 4-SL phase has instabilities at the wave-vectors $(\pi \pm \pi/3)\mathbf{x}$. The SW intensity at the larger of these two wave-vectors always dominates and the 4-SL phase evolves into cycloid II with wavenumber $4\pi\mathbf{x}/3$.

In region 4-SL I, the 4-SL phase has three unique SW instabilities: one at wave-vector \mathbf{k}_1 along the \mathbf{x} axis, another at \mathbf{k}_2 rotated by $\pi/3$, and a third at \mathbf{k}_3 rotated by $-\pi/3$. All three have the same magnitude with $\pi/2 < k_i < \pi$. Other SW instabilities in the 4-SL I re-

gion can be related by a symmetry operation to one of these three. We find that the instability at \mathbf{k}_1 always has a larger intensity than the “twins” at \mathbf{k}_2 or \mathbf{k}_3 or than any of the other wave-vectors related by symmetry. Correspondingly, cycloid I along any diagonal in Fig. 3 has the same wave-vector \mathbf{q} as the dominant instability of the 4-SL phase.

Similar conclusions are reached for the 8-SL phase, which switches to cycloid I along any diagonal in Fig. 3. Although the SW instability of the 8-SL phase occurs simultaneously at several wave-vectors, the dominant wave-vector instability of the 8-SL phase coincides with the wave-vector \mathbf{q} of cycloid I along any diagonal in Fig. 3.

However, the CNC phase that intercedes between the

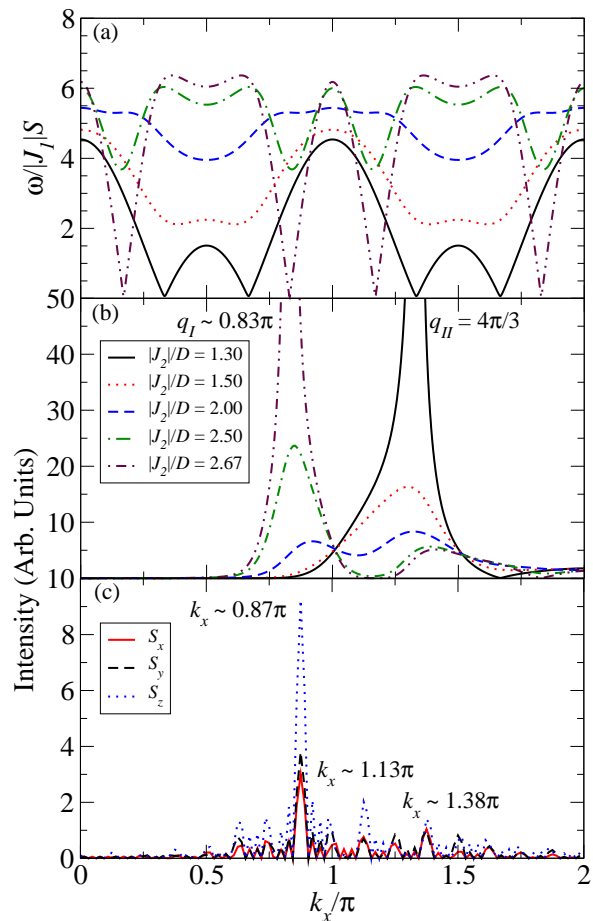


FIG. 4: (Color online)(a-b) SW frequency and intensity versus wave-vector k_x for the 4-SL phase with $|J_1|/D = 5.5$, $J_3 = 1.3J_2$, where $|J_2|/D$ varies from 1.30 to 2.67. (c) Fourier transform for the S_x , S_y , and S_z components of the CNC phase with the same exchange parameters as above and $|J_2|/D = 2.5$.

TABLE I: Energy Coefficients for Collinear, Cycloid, and CNC Phases

| Phase | A_1 | A_2 | A_3 | A_D |
|------------|---------------------------|----------------------|--------------------------|-------------|
| 4-SL | 1 | -1 | 1 | 1 |
| 8-SL | 0 | 1 | 1 | 1 |
| Cycloid I | $-(\cos(q) + 2\cos(q/2))$ | $-(1 + 2\cos(3q/2))$ | $-(\cos(2q) + 2\cos(q))$ | 1/2 |
| Cycloid II | 3/2 | -3 | 3/2 | 1/2 |
| CNC | 0.595±0.001 | -0.097±0.001 | 1.161±0.001 | 0.712±0.001 |

4-SL and cycloid I phases is characterized by several elastic peaks shown in Fig. 4(c). Within the precision of our MC simulations, the dominant wave-vector $k_x \approx 0.87\pi$ of the CNC phase coincides with the dominant instability wave-vector of the 4-SL phase that precedes it.

To demonstrate how the magnetic ground state evolves from cycloid II into the 4-SL phase and then into cycloid I, we plot in Fig. 4(a) and (b) the SW frequencies and intensities versus wave-vector for the 4-SL phase with $J_1/D = -5.5$, $J_3/J_2 = 1.3$, and $|J_2|/D$ varying from 1.30 to 2.67. As $|J_2|/D$ approaches the lower limit for the stability of the 4-SL phase, the SW intensity dominates at the cycloid II wave-vector $\mathbf{q} = 4\pi\mathbf{x}/3$. At the upper limit, the SW intensity dominates at the cycloid I wave-vector $\mathbf{q} \approx 0.83\pi\mathbf{x}$. Hence, the wave-vector of the SW instabilities for the collinear phases correspond to the ordering wave-vectors of the non-collinear phases.

Bear in mind that the transition between magnetic ground states is not always signaled by the softening of a SW mode. In fact, the transition between the 4-SL and 8-SL phases in Fig. 1 occurs even at $D = \infty$, when the spins are Ising variables and the SW gaps for both phases diverge.

The CNC phase may be related to the multi-ferroic phase observed in Al-doped CuFeO₂ [3], which was recently investigated by Nakajima *et al.* [17]. Based on neutron-scattering measurements, those authors concluded that the ground state is a modified cycloid with the same spin on sites \mathbf{R} and \mathbf{R}' (see above). This phase has peaks at wave-vectors on either side of $\pi\mathbf{x}$, in agreement with the neutron measurements. However, a modified cycloid cannot be stabilized by a Hamiltonian with the form of Eq.(1), regardless of the exchange and anisotropy parameters. With an additional phase slip δ for the spins at sites \mathbf{R}' , a pure cycloid with $\delta = 0$ and a single elastic peak always has lower energy than the phase proposed in Ref.[17] with $\delta = -q/2$. This conclusion has been verified by MC simulations.

Like the non-collinear phase proposed earlier [17], the CNC phase also contains FM correlations between sites \mathbf{R} and \mathbf{R}' or \mathbf{R}'' . So the CNC phase also has elastic peaks on either side of $\pi\mathbf{x}$ at $k_x \approx 0.87\pi$ and 1.13π , as shown in Fig. 4(c). Because the FM correlations are not perfect and vary along the \mathbf{x} direction, the CNC phase contains several other elastic peaks that may allow it to be experimentally distinguished from the phase proposed

in Ref.[17].

To summarize, we have shown that the dominant wave-vector of a non-collinear phase in a frustrated TLA corresponds to the dominant instability wave-vector of a collinear phase as the anisotropy is lowered and spin fluctuations become softer. The CNC phase sketched in Fig. 2 is a more reasonable candidate for the multi-ferroic phase observed in Al-doped CuFeO₂ than the one previously proposed.

This research was sponsored by the Laboratory Directed Research and Development Program of Oak Ridge National Laboratory, managed by UT-Battelle, LLC for the U. S. Department of Energy under Contract No. DE-AC05-00OR22725 and by the Division of Materials Science and Engineering and the Division of Scientific User Facilities of the U.S. DOE.

-
- [1] Z. Fang *et al.*, *Phys. Rev. Lett.* **84**, 3169 (2000).
 - [2] W. Zheng *et al.*, *Phys. Rev. B* **75**, 184418 (2007).
 - [3] N. Terada *et al.*, *J. Magn. Magn. Mat.* **272-276**, e997 (2004); N. Terada *et al.*, *Phys. Rev. B* **70**, 174412 (2004); N. Terada *et al.*, *J. Phys.: Cond. Mat.* **19**, 145241 (2007).
 - [4] See, for example, *Frustrated Spin Systems* (World Scientific, New Jersey, 2004), edited by H. T. Diep.
 - [5] T. Takagi and M. Mekata, *J. Phys. Soc. Jpn.* **64**, 4609 (1995).
 - [6] S. Mitsuda *et al.*, *J. Phys. Soc. Jpn.* **60**, 1885 (1991).
 - [7] M. Mekata *et al.*, *J. Phys. Soc. Jpn.* **12**, 4474 (1993).
 - [8] F. Ye *et al.*, *Phys. Rev. Lett.* **99**, 157201 (2007).
 - [9] R. S. Fishman *et al.*, *Phys. Rev. B* **78**, 140407 (2008).
 - [10] R. S. Fishman, *J. Appl. Phys.* **103**, 07B109 (2008).
 - [11] T. Kimura *et al.*, *Phys. Rev. B* **73**, 220401(R) (2006).
 - [12] S. Kanetsuki *et al.*, *J. Phys.: Cond. Mat.* **19**, 145244 (2007).
 - [13] S. Seki *et al.*, *Phys. Rev. B* **75**, 100403(R) (2007).
 - [14] M. Swanson, J.T. Haraldsen, and R.S. Fishman, (*unpublished*).
 - [15] Due to the anisotropy, the cycloids will be slightly distorted by the tilting of the spins towards the $\pm z$ directions with an energy gain of order $D^2 S^2 / z |J_1|$ ($z = 6$ is the number of nearest neighbors). Within the precision of our MC simulations, this distortion is undetectable and a pure cycloid is obtained.
 - [16] Th. Jolicoeur *et al.*, *Phys. Rev. B* **42**, 4800 (1990).
 - [17] T. Nakajima *et al.*, *J. Phys. Soc. Jpn.* **76**, 047309 (2007).